



Cite this: *Phys. Chem. Chem. Phys.*,
2024, 26, 679

Polymer mechanochemistry: from single molecule to bulk material

Qifeng Mu ^a and Jian Hu ^b

The field of polymer mechanochemistry has experienced a renaissance over the past decades, primarily propelled by the rapid development of force-sensitive molecular units (*i.e.*, mechanophores) and principles governing the reactivity of polymer networks for mechanochemical transduction or material strengthening. In addition to fundamental guidelines for converting mechanical energy input into chemical output, there has also been increasing focus on engineering applications of polymer mechanochemistry for specific functions, mechanically adaptive material systems, and smart devices. These endeavors are made possible by multidisciplinary approaches involving the development of multifunctional mechanophores for mechanoresponsive polymer systems, mechanochemical catalysis and synthesis, three-dimensional (3D) printed mechanochromic materials, reasonable design of polymer network topology, and computational modeling. The aim of this minireview is to provide a summary of recent advancements in covalent polymer mechanochemistry. We specifically focus on productive mechanophores, mechanical remodeling of polymeric materials, and the development of theoretical concepts.

Received 29th August 2023,
Accepted 30th November 2023

DOI: 10.1039/d3cp04160c

rsc.li/pccp

1. Introduction

Polymers, such as rubber, elastomer, and gel, are widely used in various everyday applications including gloves, tires, packaging materials, coatings, contact lenses, medical devices, flexible electronics, and engineering composites, due to their light-weight nature and unique mechanical properties such as high mechanical strength, toughness, elasticity and processability.^{1–3} Understanding the influence of external mechanical force on the stability and properties of polymeric materials has long been an important field of study for determining their in-use performances.^{4–6} Macroscopic mechanical forces applied to polymeric materials like stretching, indentation, compression and shear loading are known to be transferred to an individual elastically active chain, resulting in various physical and chemical reactions such as scission of covalent bonds and noncovalent interactions.^{7–9} Presently recognized as an established interdisciplinary field of polymer science, mechanics, and solid-state chemistry, polymer mechanochemistry has witnessed numerous landmark research discoveries in the last two decades.^{10–12} Polymer mechanochemistry is classified as a branch of chemistry that investigates chemical physical phenomena, such as chemical

process, crack propagation, and material toughening in aggregate states. This discipline runs parallel with other well-established branches of chemistry and soft matter mechanics, such as thermochemistry, photochemistry, and fracture mechanics.

The macromolecular response of synthetic polymeric materials to external mechanical force was first investigated by Staudinger and his co-workers in the 1930s.^{13,14} The response of polymeric materials to mechanical force can range from simple conformational changes to bond-stretching and bond-bending deformations. When subjected to sufficient mechanical force (*i.e.*, a few nanonewtons), covalent bonds undergo scission, resulting in reduced molecular weight, viscosity, and strength.¹⁵ Sohma *et al.* later experimentally demonstrated the homolytic scission of C–C covalent bonds along the polymer mainchain under mechanical force would produce radicals, using the electron spin resonance (ESR) observation.^{16,17} Early works in polymer mechanochemistry mainly focused on studying the mechanochemical degradation of polymeric materials. However, recent developments have shown a clear shift from being “destructive” to “productive” in new polymer mechanochemistry, centered around concepts such as “mechanophore”, “mechanically adaptive material system”, “mechanochemical gating”, and “mechanochemical remodeling of polymer”. Polymer mechanochemistry has the potential to serve as a powerful tool for bridging microscopic molecular scission with macroscopic material properties (Fig. 1). Several review articles and books have comprehensively summarized the advancements in various types of mechanoresponsive polymeric materials and mechanochemical polymer synthesis.^{18–24} However, on-going efforts

^a RIKEN Center for Emergent Matter Science, 2-1 Hirosawa, Wako, Saitama 351-0198, Japan

^b State Key Laboratory for Strength and Vibration of Mechanical Structures, Department of Engineering Mechanics, Xi'an Jiaotong University, Xi'an 710049, P. R. China. E-mail: hujian@mail.xjtu.edu.cn

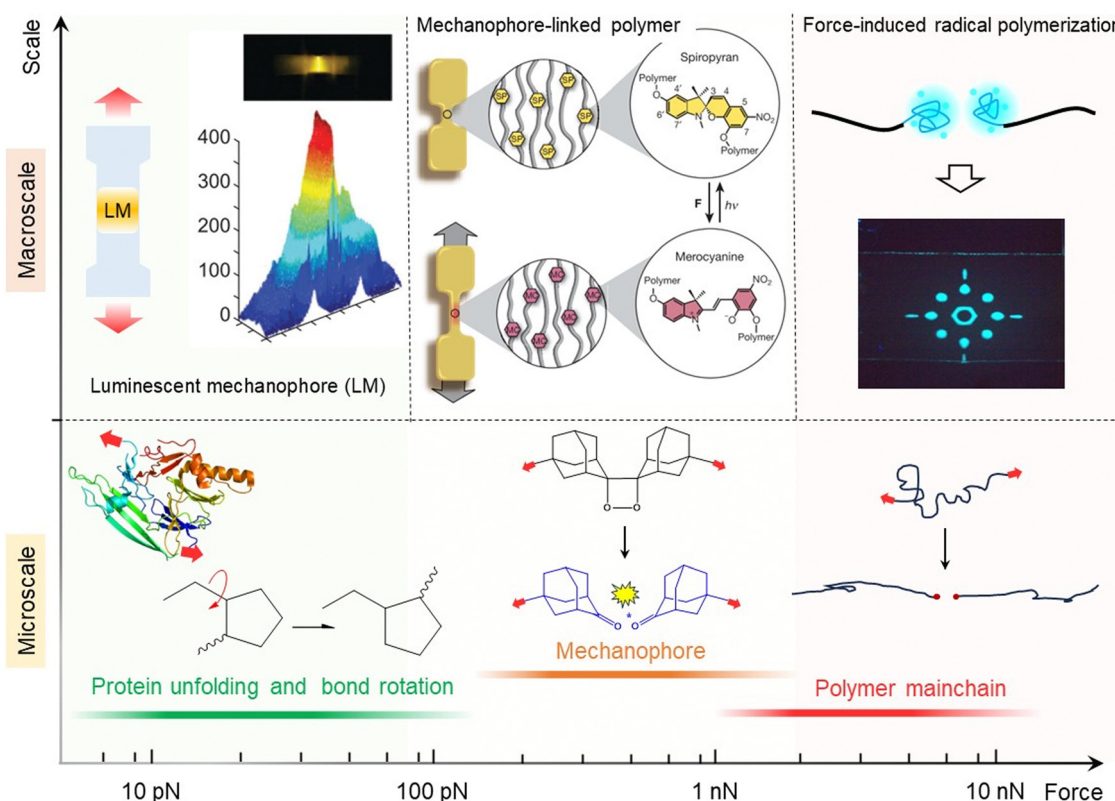


Fig. 1 Mechanical force scale for a range of macromolecular deformation and fracture processes, and changes in macroscopic properties (color and luminescence) of polymeric materials induced by the mechanical response of microscale mechanophores. Reprinted with permission from Y. L. Chen *et al.* Copyright © 2012, Springer Nature Limited; reprinted with permission from Douglas A. Davis *et al.* Copyright © 2009, Macmillan Publishers Limited. All rights reserved.

continue to inspire significant progress in this field. We firmly believe that the future direction lies in the development of novel mechanochemically responsive polymeric materials, as well as exploring their advantageous applications in toughening materials through force-triggered ring-opening reactions, free radical reactions, and click reactions. Furthermore, it is highly worthwhile exploring the synthesis of new mechanochromic moieties and their incorporation into polymer networks, investigating the mechanisms of molecular force transmission within bulk polymer, and elucidating the physical mechanisms governing crack tip stress distribution. Simultaneously, we acknowledge that understanding the thermodynamics and force-coupled kinetics of mechanochemical reactions in solid-state polymer remains a challenging endeavor.

Here we present a comprehensive yet accessible overview of the history of polymer mechanochemistry, along with recent advancements and on-going research efforts in this field. We also discuss the reasonable design of polymer network topology, placing emphasis on networks with well-designed and hierarchical structures that facilitate mechanical force transfer and mechanochemical reactions. Additionally, we also briefly introduce the computational approaches developed for studying the fracture behavior of mechanophores under mechanical loading, such as the constrained geometries for simulating external force (COGEF) based on density functional theory and the external force explicitly included (EFEI) method.

2. Mechanochemical remodeling polymeric materials

2.1. Self-strengthening

The mechanical responses of polymeric materials are dependent on the physical and chemical structures of polymer strands. Most polymeric materials exhibit viscoelastic behavior, which combines characteristics of both solids (elasticity) and liquids (viscosity). In engineering applications, polymeric materials are susceptible to mechanical damage caused by excessive stretching, compression, fatigue, and wear *etc.* Consequently, these synthetic materials often experience degradation or failure due to mechanical forces. The degradation process is associated with the scission of covalent bonds within polymer networks. Essentially, breaking a covalent bond is a chemical reaction.

In recent decades, Prof. Moore's group has drawn inspiration from early explorations in "mechanophores", and has successfully developed polymer backbones containing mechanically labile bonds by introducing these mechanical force-sensitive molecular entities.²⁵ Furthermore, Prof. Craig's group was the first to report on mechanochemical strengthening triggered by high shear force both in solution. These researchers proposed a new concept known as activated remodeling *via* mechanochemistry (ARM).²⁶ They chose *gem*-dibromocyclopropane (gDBC, 1_{closed}) as the mechanophore embedded within a poly(butadiene) backbone.

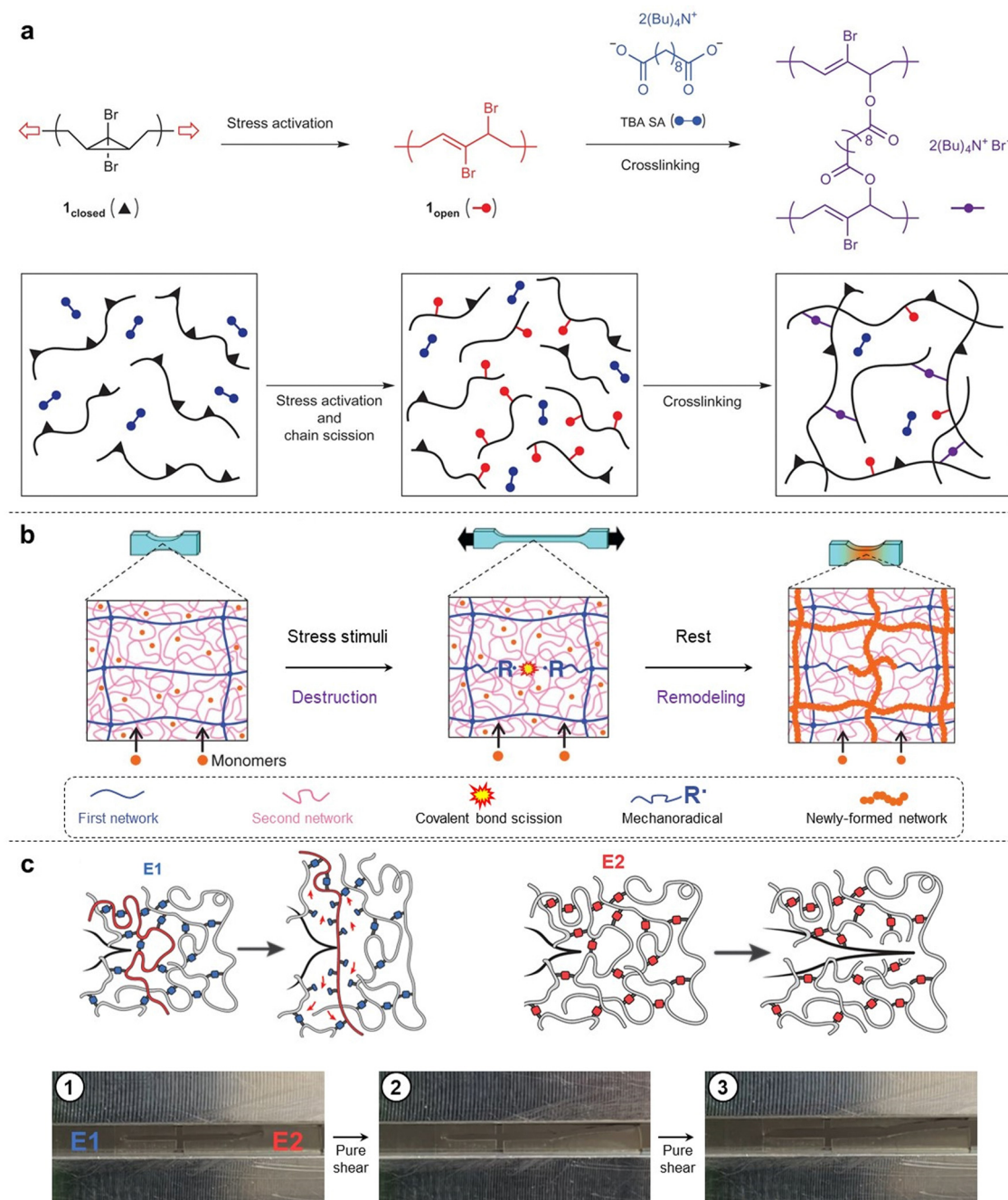


Fig. 2 (a) A gDBC mechanophore within a polymer chain under sonication undergoes a ring-opening reaction to produce an allylic bromide capable of self-strengthening through nucleophilic displacement reactions; Copyright © 2013, Springer Nature Limited. (b) The strategy to develop self-growing materials based on mechanical training of DN gels; Copyright © 2019, The American Association for the Advancement of Science. (c) Mechanically weak cross-linkers can increase the tortuosity of the crack path in elastomer 1 (E1). In contrast, cross-linkers are similarly strong as the primary chains in elastomer 2 (E2), but cannot toughen the bulk polymer; Copyright © 2023, The American Association for the Advancement of Science.

Mechanical extrusion and sonication were conducted on the macromolecules containing gDBC, which underwent a 2-electron electrocyclic ring-opening reaction to turn into the 2,3-di-bromoalkene product (1_{open}). Subsequently, the 1_{open} reacted with di-tetrabutylammonium salt of sebacic acid (TBA SA) *via* nucleophilic displacement, resulting in stable covalent crosslinking networks and orders-of-magnitude increases in bulk gel moduli (Fig. 2a). In this work, preference was given to

covalent crosslinking over polymer chain scission, ultimately achieving a transition from destructive to productive self-strengthening. This molecular-scale remodeling has a positive and dramatic impact on the bulk mechanical properties. More importantly, the use of polymer mechanochemistry provides access to a diverse range of chemical responses in solid-state systems that are often inaccessible *via* thermal and/or photochemical stimuli.

In 2015, Prof. Craig's group presented a second self-strengthening system based on mechanophore benzocyclobutene (BCB).²⁷ The BCB, embedded within the polymer strands, was proved to undergo mechanical activation and achieved interchain cross-linking *via* a Diels–Alder reaction. Therefore, they synthesized a polymer with multiple BCB units, resulting in an increase in molecular weight M_n over sonication time in tetrahydrofuran (THF) solution; however, no bulk organic gel was formed in the system. Upon the addition of bismaleimide cross-linker at the same concentration, faster gelation compared to the initial system was observed. Operating above the overlap concentration increases the likelihood of arylide on one polymer chain reacting with an alcohol on another chain to form a cross-linkage and consequently leading to a net increase in molecular weight. Unlike the previous mechanically triggered gelation system utilizing the *g*DBC-based polymer, this BCB-based cross-linking does not require any ionic components and represents an attractive alternative platform for developing mechanical force-strengthening materials. By employing the mechanoresponsive moiety hexarylbiimidazole (HABI), Prof. Sijbesma and co-workers also showed that mechanochemically generated radicals in a polymer matrix can be used for force-sensing due to the formation of colored triphenylimidazolyl (TPI) radicals, as well as for initiating secondary radical reactions.²⁸ The incorporation of the HABI mechanophore combines both color reporting of bond scission and reinforcement of the polymer matrix in a single molecular moiety. This proof of concept significantly contributes to our fundamental understanding of how researchers can manipulate the destructive nature of mechanical force to perform constructive chemistry, suggesting that force-triggered crosslinking with the HABI mechanophore may have broader applications when combined with non-volatile acrylate and thiol species.

The aforementioned attempts to remodel polymer architectures by mechanical force rely on ultrasonication-activated cross-linking reactions. In most organic solutions, the solvodynamic shear field serves as the source of mechanical force. However, achieving repeated improvement in the mechanical properties of bulk solid-state materials by directly employing these molecular mechanisms remains a challenging task. In 2019, Prof. Gong's group proposed a bio-inspired strategy based on biological metabolism to develop a self-growing hydrogel. By using a tough double-network (DN) hydrogel, they successfully created a self-growing system that gains strength and mass under repetitive mechanical stretching, achieved by coupling mechanical stimuli with substance supply from an external aqueous solution (Fig. 2b).²⁹ The key challenge in this system is to generate a sufficient number of mechanoradicals without causing catastrophic failure of the bulk hydrogel. DN hydrogel is an excellent soft material that can bridge the gap between molecular mechanisms and mechanically adaptive properties. Structurally, the DN gel comprises two interpenetrating networks with contrasting structures and mechanical properties. The first network is highly crosslinked and pre-stretched, acting as a rigid but brittle skeleton. The second network is sparsely crosslinked and relatively concentrated, acting as a soft and stretchable matrix. Owing to this load-sharing topology, numerous strands in the first network

break during deformation without causing catastrophic failure of the gel bulk, because the second network will carry load and redistribute stress once partial strands in the first network break. Typically, fracture of these first network strands occurs because of homolytic scission of covalent bonds, which generates enough mechanoradicals in DN systems (typically $\sim 10^{-5}$ M).

Although this radical concentration exceeds the minimum critical value ($\sim 10^{-8}$ M) required for radical reactions capable of inducing radical polymerization in bulk gel, further increasing the mechanoradical concentration would expand their potential applications. In 2022, Prof. Gong's group demonstrated an azoalkane-crosslinked DN hydrogel in which the mechanoradical concentration can reach a maximum value of ~ 220 μ M. This value is 5 times that of DN gels crosslinked by the traditional crosslinker *N,N'*-methylenebis(acrylamide). This enhancement can be attributed to the notably lower bond rupture force of the C–N bond adjacent to the azo group (~ 1 nN, density functional theory (DFT) simulation), compared with the traditional C–C bond or C–N bond in the amide group (~ 3 nN, DFT simulation).³⁰ In an extension of the work on self-growing hydrogels, Prof. Gong's group constructed a circulatory system for a continuous supply of chemical species to a channel containing DN hydrogels (c-DN gels), the DN gel obtains continuous remodelling or growth in response to repetitive mechanical stimuli.³¹

The mechanochemical self-strengthening field has gradually attracted more attention from researchers, Prof. Otsuka and co-workers also developed a similar self-strengthening and mechanochromic polymer system based on the mechanophore difluorenlylsuccinonitrile (DFSN). The colorful cyanofluorene (CF) radical, induced by the scission of DFSN, exhibits sufficient oxygen tolerance to be used in ambient air without any special treatment. It also demonstrates enough reactivity toward acrylate and methacrylate monomers for initiating their radical polymerization, enabling bulk polymer with a self-strengthening capability.³² The diselenide bond (Se–Se) is also an important dynamic unit that can undergo the metathesis reaction with the generation of radicals under external stimuli such as light, γ -rays, oxidation, and mechanical pressure.^{33–35} Prof. Chen and Prof. Xu's group demonstrated that sonication and mechanical compression could trigger the Se–Se bond scission to generate polymeric seleno radicals.^{36,37} These novel polymers were able to damage-report and self-strengthen synergistically under mechanical loading. Moreover, it is worth noting that mechanical sonication allows selective activation of the dynamic covalent Se–Se bond, in which the covalent bond scission occurs more rapidly for long polymer chains and is not that effective for small molecules.³⁶ In 2021, Prof. Esser-Kahn's group reported a mechanically adaptive composite system achieved through vibration-induced crosslinking. This special composite material is capable of adjusting its elastic modulus in response to external mechanical stimuli, including force, time and frequency of mechanical agitation. By utilizing a method of mechanical polymerization, the adaptive composite selectively self-strengthens, resulting in an impressive $\times 66$ increase in modulus. The researchers incorporated inorganic

mechanophores, specifically ZnO, which exhibit piezoelectric properties and respond to mid-range-frequency vibrations generated by an electrodynamic system. Remarkably high monomer conversion (95%) was achieved during the efficient mechanochemical reaction process, suggesting kinetics similar to the step-growth polymerization in solid-state polymer. Furthermore, this composite material demonstrated structural adaptation along the distribution of mechanical forces, resembling the behavior observed in human bone remodeling processes where biological materials adapt according to loading locations.³⁸

Recent advances in polymer mechanochemistry now enable the synthesis of polymer strands that extend the covalent bonding along their backbone when stretched. In 2021, Prof. Craig and collaborators reported a special polymer network design in which the constituent strands lengthen through force-coupled mechanochemical reactions that are triggered as the strands reach their threshold force. In comparison with polymer networks made from analogous control strands, these reactive strand extensions of up to 40% lead to hydrogels that can stretch an additional 40–50% and exhibit tear energies twice as large. In this work, the researchers proposed a novel concept called reactive strand extension (RSE), which involves both cyclobutene and stored length in the first network to toughen the whole bulk hydrogel.³⁹ It is worth mentioning that a similar non-covalent expansion system was reported by Prof. Guan *et al.* before this work.⁴⁰ In principle, the strand extension is provided by sodium salts of bicyclodecane (BCD) mechanophores, which react through force-coupled cycloreversion to release stored length. This ingenious topological design and force-triggered ring opening at the single molecule level enable macroscopic toughening of bulk materials. Unlike incorporating weak, reversible physical cross-linking or noncovalent interactions, this enhancement does not come with a concomitant increase in the viscous modulus of the polymer strands, as evidenced by the overlap of repeated unloading-loading cycles at the same maximum strain. Here, mechanical energy dissipation is only triggered when necessary for fracture resistance and does not need to be overcome during routine functions of soft materials when fracture is not imminent.

Mechanically weak bonds, such as hydrogen bonds and ionic bonds, have been widely applied to toughen polymer networks. However, it has also been demonstrated that covalent bonds can effectively toughen polymer networks. Prof. Otsuka's group successfully demonstrated the sacrificial dynamic cross-linking capabilities of a mechanophore called difluorenyl-succinonitrile (DFSN), which not only possesses mechanochromic properties but also aids in visualizing cleavage events within polymer networks.³² Their findings shed light on failure mechanisms associated with covalently cross-linked polymers and represent a significant advancement in fundamental research on polymer chemistry and its applications in material toughening. Prof. Yang's group developed an ambient-stable dynamic covalent bond C–N with reversible stress-responsiveness in real time, providing a useful strategy for designing covalently crosslinked poly(methyl acrylate) based polymers

with multiple force-responsive functions. These materials exhibit enhanced mechanical toughness and ductility, adaptability to dynamic engineering environments, and network autonomy. Therefore, the ambient force-reversible C–N covalent crosslinking can be considered as a novel dynamic molecular platform for designing high-performance polymeric materials.⁴¹

In 2023, Prof. Craig's group demonstrated that cyclobutane-based mechanophore cross-linkers can break through force-triggered cycloreversion, leading to networks that exhibit up to nine times higher toughness compared to conventional analogs. The researchers proposed that this mechanical response is attributed to a combination of strong and long primary polymer strands, along with cross-linker scission forces that are approximately fivefold smaller than control cross-linkers at the same timescales. Furthermore, this enhanced toughness is achieved without the presence of hysteresis commonly associated with noncovalent cross-linking, and the toughening effect is universal for elastomers and gels. Through their experimental systems, it has been proven again that material properties strongly depend on the force-coupled reactivity of the mechanophore. A molecular dynamics simulation of network fracture under uniaxial stretching provides a physical picture: at high strain around the crack tip, mechanochemically weak cross-linkers in elastomer exclusively break while leaving the primary chain bonds intact, and relevant elastically active strands between cross-linkers thus become much longer compared to those in the control example (Fig. 2c).⁴² Here, the macroscopic properties of bulk polymer can be directly correlated with force-triggered molecular reactivity and mechanisms. Fracture in cross-linked networks is productively viewed as a sort of “molecular composite”, and that physical picture has implications for the use of “weak” bonds to strengthen covalent polymer networks.

2.2. Force-triggered surface grafting and patterning

The surface microstructures and chemical properties of polymeric material are crucial for biomedical engineering, tough adhesion, soft sensor, and flexible electronics. Various techniques have been employed to graft functional molecules or create patterns on polymer surfaces, including thermochemistry, electrochemistry, and photochemistry.

It poses a significant challenge to physically and chemically remodel the soft and wet surface of DN hydrogels due to the absence of chemical modification sites on the gel surface, as well as the failure of molding and photolithography resulting from the two-step synthesis process. However, in nature, functional microstructures on creature surfaces are usually formed through a surface growth mechanism. Taking inspiration from this self-growing phenomenon, Prof. Gong's group pioneered a force stamp method for growing microstructures on hydrogel surfaces based on a force-triggered polymerization mechanism of DN hydrogels. The controlled breaking of stress/strain-induced covalent bonds on the DN hydrogel surface ensures spatially controllable surface remodeling.⁴³ To realize the force-triggered surface microstructure growth, the researchers first successfully prepared a DN structure at the surface using a surface-bulk transition strategy.^{44,45}

In contrast to a nearly elastic single-network (SN) hydrogel made of polyacrylamide (PAAm), which exhibits negligible mechanical hysteresis upon cyclic indentation, the tough DN hydrogel surface shows obvious hysteresis, indicating energy dissipation by the rupture of covalent bonds in the first network. To directly verify that cyclic indentation induces internal fracture near the surface layer of DN hydrogels, optical microscopy was employed to observe damage zones on their surface. According to the Lake–Thomas theory, when the indentation depth is 1000 μm , the estimated mechanoradical concentration is 2.9×10^{-5} M. To realize surface microstructure growth, DN hydrogels were immersed in aqueous solutions containing different monomers. First, a fluorescent molecular probe of 8-anilino-1-naphthalenesulfonic acid (ANS)^{46,47} was used to visualize the newly formed regions of poly(*N*-isopropylacrylamide) (PNIPAm) inside and on the DN gels, thereby confirming force-triggered radical polymerization (Fig. 3a). Additionally, the authors studied the monomer conversion ratio during the force-triggered radical polymerization by comparing changes in monomer concentration within gel bulk before and after sample stretching. The results reveal that 2-acrylamido-2-methylpropanesulfonic acid sodium salt (NaAMPS) exhibits the highest conversion ratio $\sim 80\%$, while *N*-isopropylacrylamide (NIPAm) displays a higher conversion ratio of $\sim 69\%$ compared to acrylic acid (AAc), sodium *p*-styrenesulfonate (NASS), and 3-(methacryloylamino)propyltrimethylammonium chloride (MPTC). Furthermore, complex microstructures at different scales can be created

on DN hydrogels using the proposed force stamp method. As proof-of-concept examples, two interesting applications of these hydrogels with the force-triggered growth of surface microstructures were demonstrated. Firstly, it is shown that these surface microstructures provide chemical cues for inducing highly oriented mouse myoblast cells. Moreover, anisotropic DN hydrogel surfaces with parallel PNIPAm patterns are capable of regulating surface wettability and water droplet directional transportation. This spatially controllable force-triggered growth method allows precise modulation of microstructure size and shape. Unlike conventional light-triggered growth limited to photoactive substrates, this force-triggered growth is not restricted to DN gels but can potentially be applied to various types of multiple-network polymeric materials.

Mechanochemical activation of covalent bonds within bulk polymers typically occurs with irreversible deformation of the substrate material. Using a colorimetric mechanophore spiro-pyran, Prof. Craig and co-author Prof. Zhao developed an electro-mechano-chemically responsive (EMCR) elastomer system to show that bond activation can be repeated over multiple cycles of tensile elongation with full shape recovery.⁴⁸ The mechanochromic elastomer is fabricated by covalently incorporating the mechanophore spiropyran into the cross-linked network of the silicone elastomer Sylgard 184. Unlike most mechanophore-bearing polymeric materials that typically undergo plastic deformation or mechanical fracture upon external mechanical stimuli, this study utilizes electric fields to induce various

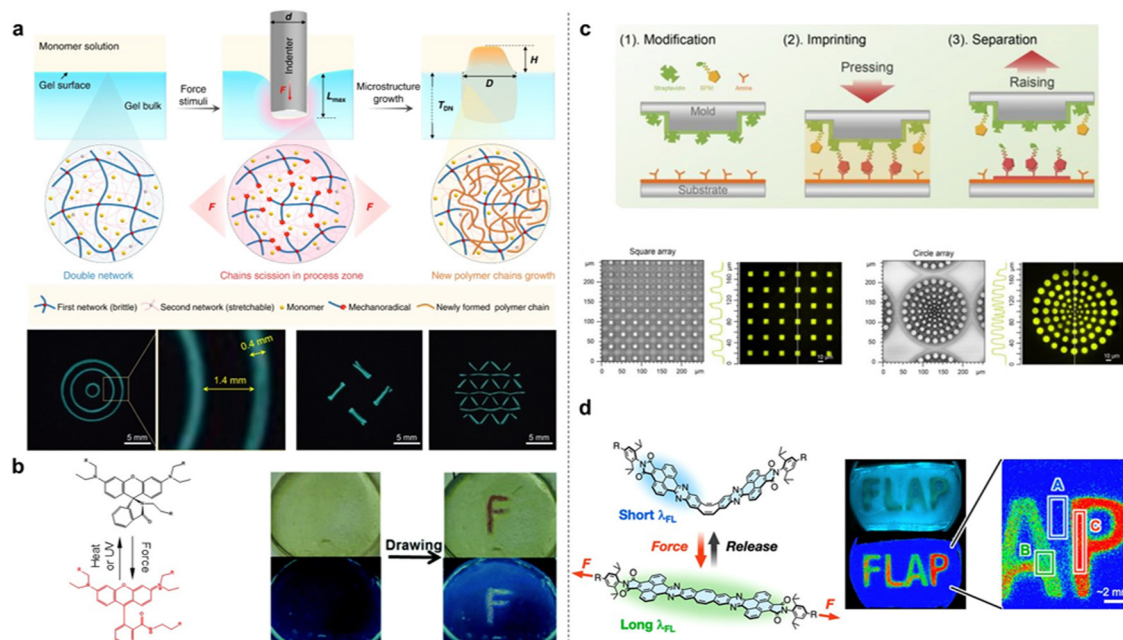


Fig. 3 (a) A mechanochemical strategy to rapidly grow various microstructures on a DN hydrogel surface; Reprinted with permission from Q. F. Mu et al., Copyright © 2022, All rights reserved. (b) Activation of rhodamine and the reverse reactions by stimulation with external force and heat or UV, where rhodamine was embedded into elastomer film, which was drawn and showed a color change; Copyright © 2015 Wiley-VCH Verlag GmbH & Co. KGaA, Weinheim. (c) Schematic of the mechanochemical lithography process in fabricating the biotin array, and a fluorescence image of the produced pattern; Copyright © 2022, American Chemical Society. (d) Conformational change of a structurally modified flapping force probe (FLAP) which enables a real-time ratiometric fluorescence, photographs (RGB) and stress mapping of gel compressed by a metal stamp; Copyright © 2022, American Chemical Society. All rights reserved.

fluorescent patterns (lines, circles, letters, *etc.*) of large deformation on the elastomer substrate. It is the first time that these on-demand fluorescent patterns have been achieved by integrating the EMCR elastomer into a display panel controlled by applied electric fields. The mechanical activation and fluorescent patterning of the EMCR elastomer are reversible and repeatable over multiple cycles. Furthermore, theoretical models are constructed to predict the electrically induced fluorescent patterns and guide the design of elastomers and smart devices in this category. Fluorescent microscope observations reveal that stress concentration zones radiate stronger fluorescent signals, due to the higher density scission of covalent bonds in those areas. The current demand for stretchable elastic materials to adapt cyclic deformation necessitates the development of novel mechanophores with reversible reactivity.

In 2015, Prof. Jia and co-workers reported a new mechanochromic and photochromic polyurethane film incorporating a mechanophore rhodamine B (Rh-B). The rhodamine-based molecule, named Rh-OH, was found to act as both a mechanophore and a photochromic compound in the stretchable polymer matrix. The mechanophore Rh-OH was designed with a tertiary amino group and two attachable points located separately on the five-membered heterocyclic ring and phenyl ring. A visible color change indicates chemical transformation of Rh-OH from twisted spirolactam to planarized ring-opened amide in an acidic environment, confirming the isomerization of Rh-OH implanted in the polyurethane.⁴⁹ Mechanoresponsive properties were confirmed by using a pen-like pestle to draw an "F" on the film surface (Fig. 3b); only scratched areas exhibited distinct reddish color under UV light in contrast to the blue surrounding regions. After annealing, new patterns emerged clearly under UV light, demonstrating the easily erasable writing characteristic of this photochromic polymer. The constrained geometries simulate external force (COGEF) method was used to calculate the activation energy for the force-triggered ring-opening reaction of Rh-OH at approximately 133.2 kJ mol⁻¹, lower than the C-C bond energy of ~350 kJ mol⁻¹. The dual-responsive film may advance the development of real-world applications for mechanochromic materials.

Recently, Prof. Cao and co-workers also developed a mechanochromic lithography (MCL) method based on compressive force-triggered reactions to prepare a special surface with patterned biomolecules.⁵⁰ In their systems, the mechanochemical inks (MCIs) consist of biomolecules containing both a bio-affinity ligand and a mechanoactive group. The presence of the mechanoactive group facilitates covalent immobilization of MCIs through compressive force-triggered reactions in an aqueous solution mixture, allowing for direct and continuous printing. By employing MCL, it is possible to achieve patterns with nanoscale spatial resolution limited only by the minimum template feature size. The resulting nano-patterns were verified by fluorescence imaging (Fig. 3c). In addition, the imprinting process can be repeated multiple times to increase the density of immobilized MCIs. They first confirmed that the ubiquitously present amino groups in biomolecules can undergo a force-triggered Michael addition with

maleimide in a vibrating ball mill. Vibrating ball milling is also commonly used as a mechanochemical synthetic method, compared to direct compression imprinting. The special MCIs such as biotinyl-maleimide and his-tagged proteins containing exposed amines were used for mechanochemical imprinting. They found that the patterned target molecules on the surface exist as a monolayer with an approximate height of 1 nm. To confirm the stability of the maleimide-amine bond, rupture forces corresponding to single-molecule events were measured by single-molecule force spectroscopy (SMFS), resulting in average rupture forces of 674 ± 355 pN (mean \pm SD) at pH 7.4 for aminosuccinimides. The rupture forces are dependent on the pH of the external aqueous solution. Furthermore, fluorescent protein arrays were covalently patterned onto substrates using the MCL method. However, it should be noted that these proposed strategies primarily take place in air, inevitably leading to drying and inactivation of biomolecules on the stamp or cantilever tip surfaces. This work opens a new avenue for patterning biomolecules using mechanochemistry. In 2021, Prof. Saito's group presented a flapping molecular force probe (FLAP), which can evaluate nanoscale forces transmitted in the polymer chain network by ratiometric analysis of stress-dependent dual fluorescence.⁵¹ The calculated force threshold for the single-molecule fluorescence switching of FLAP is approximately 100 pN, surpassing thermal fluctuation levels (4.1 pN nm). It was observed that the fluorescence response of FLAP under small stress enables the detection of local stress distribution around the crack tip. Mechanically compressing a metal stamp onto the polyurethane film allows for the creation of visually appealing fluorescent letters spelling "FLAP" (Fig. 3d).

In 2023, Prof. Robb's group introduced a novel mechanophore platform enabling mechanically gated multi-color chromogenic reactivity. The mechanophore is based on an activated furan precursor to donor-acceptor Stenhouse adducts (DASAs) masked as hetero-Diels-Alder species. Mechanochemical activation of the mechanophore unveils the DASA precursor, and subsequent reaction with a secondary amine generates intensely colored DASAs.⁵² DASAs are a recently established class of highly modular, optically tunable, and visible-light photo-switches. Mechanochemical activation of DASAs in organic solution is achieved by ultrasonication, while in solid polymers occurs under mechanical tension or compression. Following mechanical activation, the addition of various secondary amines produces a chromogenic reaction leading to distinctly colored DASAs all from a single mechanophore. Additionally, they demonstrated the versatility of this mechanochemical platform by establishing the concept of mechanochemical multi-color soft lithography for printing complex multi-color patterns on an elastic polydimethylsiloxane (PDMS) substrate.

3. Mechanophore for self-reporting materials

The mechanophores used in self-reporting material systems include two types: mechanochromic mechanophores and luminescent

mechanophores. These force-sensitive molecular units possess mechanically labile bonds. When incorporated within a mechanically stressed polymer matrix, the mechanophores undergo chemical transformations that result in color change and/or fluorescence emission. Recent developments in the field of self-reporting materials with mechanophores have mainly focused on (i) designing novel mechanophores for various applications such as stress mapping around crack tips, failure and healing detection in composite interfaces or pure polymers, *etc.*, and (ii) gaining fundamental insights into macromolecular architectures, network topology, and physical attributes of polymers that promote efficient transduction of mechanical energy into chemical transformation.

3.1. Mechanochromic mechanophores

Mechanochromic mechanophores, which are a family of artificial force-sensitive units that change their optical properties in response to external mechanical forces, play a critical role in eliciting various chemical transformations within solid-state polymer matrices. Extensive on-going efforts have been dedicated to revealing a rich library of mechanochromic mechanophores and the corresponding self-reporting systems. We believe that the mechanochromic mechanophores with immediate color

emergence and fading upon stress loading and release are suitable for monitoring temporal and online stress distribution and changes, thereby enabling a variety of potential applications.

Spiropyran (SP) is a classical mechanochromic probe that undergoes ring opening upon external loads, resulting in a distinct color change from yellow to blue, by breaking the weak bond between the nodal carbon atom and the ethereal oxygen. This ring opening process can be induced through various means such as thermal or photon absorption, selective solvation, grinding, or stretching (Fig. 4a). In 2009, Prof. Sottos's group first reported a mechanoresponsive polymeric material by directly incorporating SP mechanophores into polymer chains or cross-linking points of bulk polymers.⁵³ They employed first-principles steered molecular dynamics and constrained optimization (COGEF) simulations to model the effect of external mechanical force on the mechanophore. Control experiments demonstrated that external stress could locally activate the mechanophores linked into elastomeric or glassy polymers. The mechanically induced color change was found to be reversible after approximately 6 h of exposure to fluorescent room light. Thus, spirocyclic mechanophores serve as valuable molecular force probes for visible detection and mapping of mechanical stresses within bulk polymers. They found that activation of the mechanophore-linked

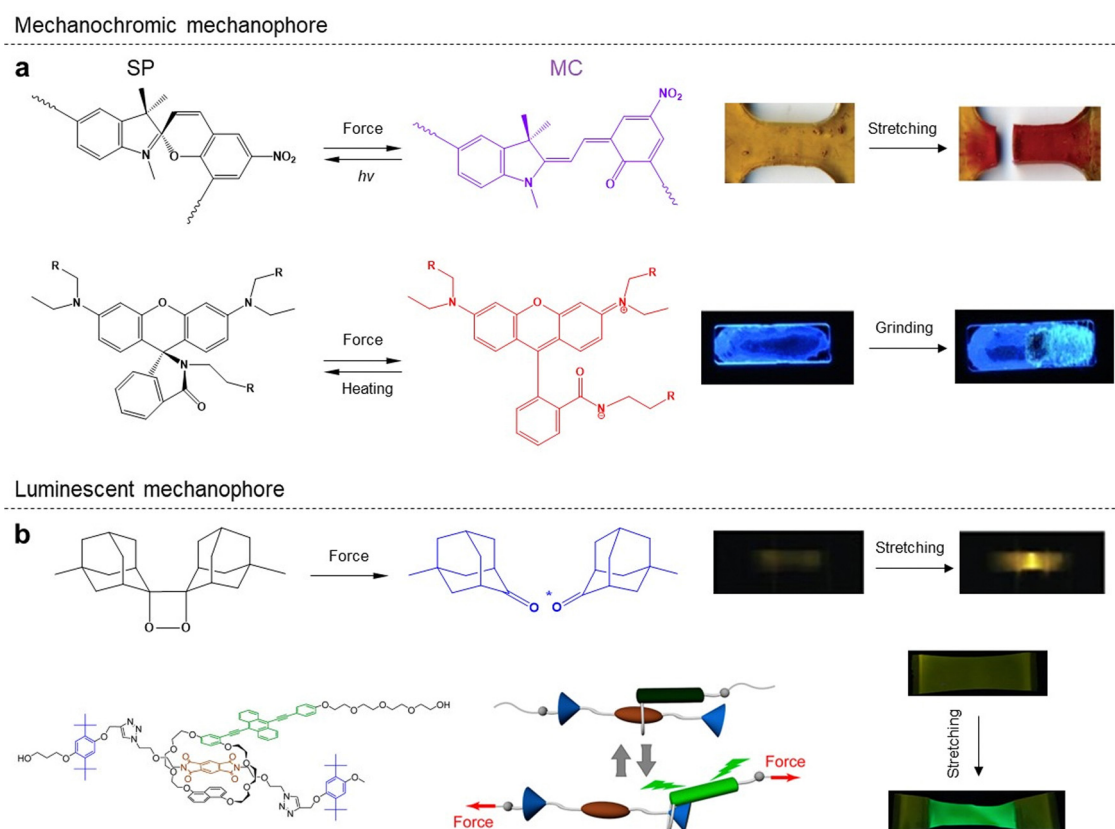


Fig. 4 (a) Under uniaxial extension, spirocyclic units were converted into highly colored merocyanine, resulting in a color change in a polymeric material, and chemical structure change of rhodamine-based molecule after grinding, resulting in a blue powder sample; Copyright © 2009, Macmillan Publishers Limited, Copyright © 2013 Wiley-VCH Verlag GmbH & Co. KGaA, Weinheim. All rights reserved. (b) A dioxetane luminescent mechanophore is activated by force and emits light, and supramolecular mechanophores are prepared by locking a fluorophore and quencher in a rotaxane. Copyright © 2012, Springer Nature Limited, Copyright © 2022, American Chemical Society. All rights reserved.

polymer was achieved when plastic flow exceeded a certain strain threshold, leading to distinctive color signatures. This molecular probe aids in understanding the effects of stress and failure on polymeric materials while providing an opportunity for assessment, modification, and improvement prior to catastrophic failure. In 2010, Prof. Scotts and co-workers demonstrated the force-induced redistribution of a chemical equilibrium of the SP mechanophore, showcasing its potential for visible detection and mapping of local stresses in bulk polymers through mechanically induced transformation into the merocyanine (MC) conformation.⁵⁴ Visible spectroscopy revealed a linear increase in absorbance with mechanical strain, while maintaining a constant strain prevented the MC form from reversing back into the thermodynamically preferred SP form, indicating a strain-induced change in the energy landscape of the SP mechanophore system. Spiropyran emerges as an excellent candidate for damage/stress sensing within bulk polymers due to its mechanochromic properties, making it an ideal model mechanophore for fundamental studies on mechanoactivation behaviors in polymer systems. Recently, SP mechanophores have been incorporated into various polymer systems such as poly(ϵ -caprolactone) (PCL) with three-dimensional (3D) printing structures to study mechanochemistry.⁵⁵

Rhodamine and its derivatives were also incorporated in a rubber-like polymer such as polyurethane, which was found to exhibit mechanochromism upon mechanical stretching. The application of polymeric networks to restrict the isomerization of rhodamine may be a step forward in the synthesis of rhodamine-based chromogenic polymeric materials.^{49,56} Diarylbibenzofuranone (DABBF), a dynamic covalent bonding group, shows great promise as a mechanochromic probe due to its capacity for undergoing homolytic bond cleavage in response to external mechanical force, resulting in the formation of colored radicals in air. In this study, the quantitative evaluation of the dynamic covalent mechanophore using electron paramagnetic resonance (EPR) spectroscopy allows for an accurate estimation of the amount of dissociated DABBF mechanophores *in situ*, providing valuable insights into fracture and fatigue mechanisms in polymeric materials.⁵⁷ Additionally, difluorenylsuccinonitrile (DFSN), a novel radical-type mechanophore with high thermal stability exhibited by its central carbon–carbon bond, can be utilized for synthesizing mechanochromic polymers through living radical polymerization. The resulting bulk polymer based on DFSN demonstrates both desirable mechanochromism and excellent thermal resistance up to 150 °C. Furthermore, the activation of DFSN-based polymers is selectively triggered by exposure to mechanical force, leading to the generation of colored radicals.⁵⁸

3.2. Luminescent mechanophores

In 2012, Prof. Sijbesma and co-workers showed that the incorporation of 1,2-dioxetane mechanophore into poly(methyl acrylate) (PMA) chains or crosslinked networks leads to the emission of visible light under mechanical force application. Sonication of solutions containing linear polymer chains with

1,2-dioxetane and straining of polymeric networks with 1,2-dioxetane crosslinkers both exhibited bright-blue luminescence (Fig. 4b).⁵⁹ The real-time camera recorded the mechanically induced emission of blue light from the bulk polymer while simultaneously measuring mechanical stress. This mechanical activation enables high temporal resolution monitoring of bond-scission events facilitated by 1,2-dioxetane. By varying the acceptor molecule, they were able to tune the emission band; the perylene resulted in green light emission while *N,N'*-bis(2,5-di-*tert*-butylphenyl)-3,4,9,10-perylene dicarboximide produced red light emission at approximately 510 nm and 650 nm respectively. The delay between triggering the mechanophore and emitting light is on a nanosecond scale. This platform holds promise for studying stress distribution in bulk polymers by manipulating both the spacing between 1,2-dioxetanes and the polymer network topology. Predictably, this novel mechanophore acts as a specific and luminescent probe capable of sensing and mapping deformations, stresses, and damage in various bulk polymers such as elastomers, plastics or rubbers.

Prof. Chen's group has reported several representative works on various luminescent mechanophores. In 2018, they demonstrated a novel strategy to enhance the mechanoluminescent sensitivity in 1,2-dioxetane-modified thermoplastic elastomer polyurethanes (PUs) by incorporating two kinds of fluorescent dyes as repeating units into the PU backbones.⁶⁰ This strategy simplifies the process of obtaining high-quality mechanoluminescent polymeric films with an increased number of acceptor units. In 2019, Prof. Chen's group developed a series of robust polyurethanes that incorporate 1,2-dioxetane and aliphatic disulfide into the backbones and confine them within the hard microphase. These novel polymer systems exhibit excellent mechanical properties, self-healing capabilities, and mechanoresponsive behaviors based on a phase-locked bond design strategy. By combining self-healing and self-reporting units in one polymer strand using this special strategy, different mechanisms involved in self-healing can be visually distinguished through bond formation and chain entanglement.⁶¹ Recently, Prof. Chen and co-workers demonstrated a mechanochemiluminescent poly(methyl acrylate) (PMA) with intense red emission, which is highly desirable in view of its strong penetrability and high resolution in red luminescence imaging applications.⁶² Their system introduces sensitized luminescence from rare-earth Eu(III) complexes into the mechanochemiluminescence from polymeric dioxetane through covalent bonding interactions. It should be noted that this red-emissive dioxetane system enables precise localization and timing of covalent bond scission events with high resolution.

Prof. Sagara and co-workers reported a rotaxane-based supramolecular mechanophore that displays both reversible and irreversible mechanical responses, depending on the magnitude of the applied force. The novel rotaxane-based mechanophores are composed of a ring featuring a luminophore, which is threaded onto an axle with a matching quencher and two stoppers. With repeated stretching, the number of dethreaded rings gradually increases, resulting in an irreversible change

in photoluminescence intensity. The overlapping strain regimes triggering reversible and irreversible responses in these materials indicate that not all mechanophores experience the same level of force.⁶³ Prof. Saito's group developed a ratiometric force probe with dual fluorescence properties, featuring rigid wings and a flexible joint. The flapping fluorophores (FLAP) with a flexible 8p ring are rapidly gaining attention as a versatile photofunctional system. This novel mechanophore allows us to monitor stress concentration at the molecular level in deformed polymer networks prior to the structural damage by covalent bond scission.⁶⁴

Several other luminescent mechanophores with associated optical emission have been implemented within a polymer matrix. Π -extended anthracene is a special fluorescent mechanophore that exhibits high intensity and quantum yield per active mechanophore.⁶⁵ It can be excited by and emits visible light, making it experimentally convenient. Unlike spiropyran, this fluorescent mechanophore operates through scission and is irreversible. Similarly, a dimeric anthracene moiety emits in the 500–600 nm range when excited with UV light.⁶⁶

4. Mechanochemical gating and chemicals release

The concept of mechanochemical gating describes a special system in which a chemical reaction occurs only when it is preceded by a mechanical force stimulus. In 2016, Prof. Craig and co-workers presented the first example of a mechanically gated reaction in which a molecule containing two distinct mechanochemically active groups underwent sequential activation under external force (*i.e.*, the second mechanophore moiety was gated by the first one).⁶⁷ In 2018, Prof. Robb's group introduced a similar concept of mechanochemically gated photo-switching using a new mechanophore based on a cyclopentadiene–maleimide Diels–Alder adduct. DFT calculations using the constrained geometries simulate external force (COGEF) method evaluate the mechanochemical activity of cyclopentadiene–maleimide adducts. The force-triggered reaction occurs with an estimated break force of 4.6 nN. It is important to note that molecule forces calculated with the COGEF technique are typically overestimated compared to experiment results; nevertheless, they provide a beneficial framework for evaluating relative mechanochemical activity. Control experiments conducted by researchers confirm that mechanical force is responsible for “unlocking” the photochromic properties of the cyclopentadiene–maleimide mechanophore.⁶⁸

Prof. Mooney and co-workers demonstrated that ultrasound does not permanently damage these materials but enables nearly digital release of small molecules, proteins, and condensed oligonucleotides. They showed that ultrasonic irradiation can trigger on-demand drug delivery *in vivo* and enhance the effects of sustained baseline release in self-healing and ionically cross-linked polymers.⁶⁹ Prof. Boydston's group described a mechanochemical transduction method that probes the activation of bonds orthogonal to an elongated polymer chain. By mechanically

compressing mechanophore-cross-linked materials, they observed the cleavage of covalent bonds that were not integral components of the elongated polymer segments, resulting in the release of small molecules. The development of flex-activated mechanophores is undoubtedly a significant success.⁷⁰ In 2014, Prof. Boydston and co-workers developed a mechanochemically responsive elastomer capable of successively releasing small molecules from a cross-linked network upon repeated compressions. In their research work, the mechanophore features an oxanorbornadiene that undergoes “flex activation”, in which bond bending motions directed by the application of mechanical stress led to the scission of bonds orthogonal to the polymer backbone *via* retro-[4+2] cycloaddition.⁷¹ In 2012, Prof. Moore's group reported a new mechanophore with acid (HCl) releasing capability, which is designed to produce a simple catalyst for chemical change in materials under mechanical compression. The availability of the released acid is confirmed by exposing a piece of insoluble compressed polymer to a pH indicator solution. This acid-releasing mechanophore extends the possibilities in autonomous self-healing material systems.⁷² In 2023, Prof. Chen and Prof. Xiao's group introduced a novel flex-activated mechanophore (FA) based on the Diels–Alder adduct of anthracene and dimethyl acetylenedicarboxylate that exhibits turn-on mechanofluorescence.⁷³ The results show that FA can release fluorescent anthracenes through a retro Diels–Alder reaction under mechanical compression or high pressure, respectively. The unique flex-activated mode with highly emissive fluorophore release enriches the structural and functional diversities of mechanoresponsive polymeric materials.

5. Mechanocatalysis and synthesis

In 2004, Prof. Sijbesma and co-workers investigated the potential of mechanical force to induce ligand dissociation from transition-metal complexes, thus presenting a novel strategy for studying and controlling the chemistry of coordination complexes. The creation of vacant coordination sites in combination with the complete reversibility of this process paves the way for its application in transition metal catalysis.⁷⁴ In 2009, Prof. Sijbesma's group demonstrated the mechanical force activation of latent metathesis catalyst. They found that silver(I) complexes containing polymer-functionalized N-heterocyclic carbenes, which act as latent organocatalysts, exhibit catalytic activity in transesterification reactions when subjected to ultrasound in organic solvents (Fig. 5a).⁷⁵ Furthermore, force activation of a ruthenium carbene complex with attached polymer chains results in catalysis of olefin metathesis reactions. The observed catalytic activity results from ligand dissociation induced by transmission of mechanical forces from the polymeric substituents to the coordination bond. Prof. Chen and co-workers have successfully synthesized a series of Se–Se-linked polystyrenes, which were then subjected to pulse sonication.³⁶ They found that sonication can serve as an alternative stimulus for cleaving the Se–Se bonds in polymers, followed by diselenide metathesis, instead of heating or light. This approach enables selective metathesis reactions

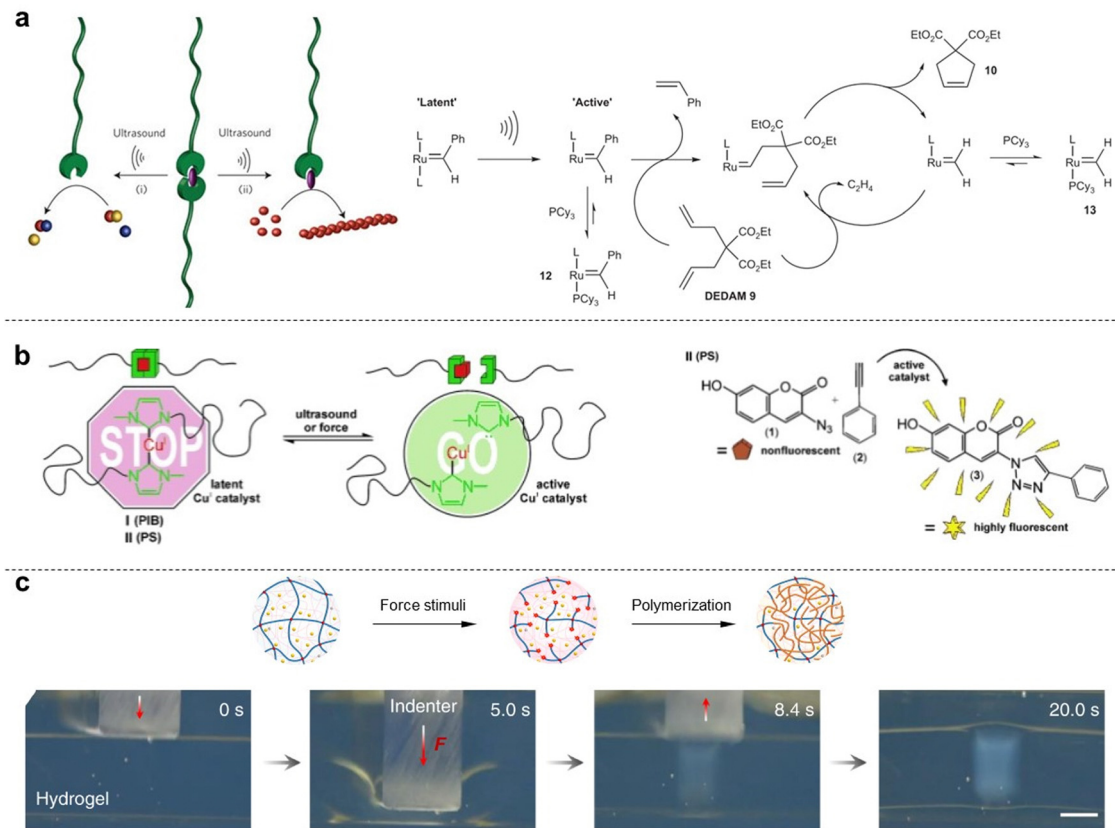


Fig. 5 (a) Concept, catalysts used and reactions of mechanical catalyst activation; Copyright © 2009, Springer Nature Limited. (b) Mechanochromic activation of latent copper(I) N-heterocyclic carbene (NHC) catalysts; Copyright © 2013 Wiley-VCH Verlag GmbH & Co. KGaA, Weinheim. All rights reserved. (c) Sequential snapshots to show the fast, regioselective force-induced polymerization of a DN gel in NIPAm solution and schematic illustration for rapid radical polymerization induced by mechanical force, scale bar is 5 mm. Reprinted with permission from Q. F. Mu *et al.*, Copyright © 2022, All rights reserved.

between diselenide-linked polymers and small molecules. Notably, benefitting from the dynamic covalent feature of Se–Se bonds, the post-sonicated polymers possess great opportunities toward chromic functional polymers through metathesis derivative reactions. Compared to the conventional stimuli, such as heating and light, the mechanochemical transduction is a remote-controlled, destructive means for therapeutics.

In 2015, Prof. Binder introduced a homogeneous Cu catalyst that can be activated through mechanical force when attached to suitable polymer chains, acting as a lever to transmit the force to the central catalytic system. Activation of the subsequent copper-catalyzed “click” reaction (CuAAC) is achieved either by ultrasonication or mechanical pressing of a polymeric material, using a fluorogenic dye for catalyst activation detection. Based on an N-heterocyclic copper(I) carbene with attached polymeric chains of different flexibility, the force is transmitted to the central catalyst, thereby activating a CuAAC in both solution and solid state (Fig. 5b).⁷⁶ In 2016, Prof. Weng's group reported that a special polymer incorporating spirothiopyran (STP) manifest both green mechanochromism and force-induced addition reactions in organic solutions and solid-state environments. In force-loaded elastic materials, colorless spirothiopyran rapidly isomerizes into green thiomerocyanine,

resulting in the observed mechanochromic effect. The presence of thiolate groups in thiomerocyanine makes it reactive toward C=C bonds, enabling the elastic material to undergo force-triggered cross-linking reactions.⁷⁷

To visually observe force-induced radical polymerization in solid-state polymers, Prof. Gong's group demonstrated an innovative approach by immersing a DN gel in a concentrated *N*-isopropylacrylamide (NIPAm) aqueous solution and pressing it with a macro-size indenter. The thermoresponsive PNIPAm show obvious turbidity and changes in the transmittance of visible light at the phase separation state.⁷⁸ The resulting turbid phenomenon, caused by the newly formed PNIPAm phase separation, implies that force-triggered polymer strand scission induces rapid radical polymerization within the gel material (Fig. 5c). Furthermore, time-resolved near-infrared spectroscopy revealed that the force-triggered radical polymerization of NIPAm was completed within seconds, consistent with the fast transparency change on a macroscale level.⁴³ These sufficient experimental evidences by *in situ* observations demonstrate the high efficiency of mechanochemical reactions in solid-state polymers, when compared with other synthetic strategies.

In some special polymer mechanochemistry systems, the external mechanical force can induce the unique mechanochemical

reaction pathways. Prof. Moore's group presented that mechanically sensitive chemical groups (*cis*-isomer) enable harnessing of mechanical forces generated during sonication of polymer organic solutions, and this mechanophore allows researchers to accelerate rearrangement reactions and bias reaction pathways to yield products not obtainable from purely light or thermal-induced reactions. The mechanical force can be used by linear polymer chains to accelerate and alter the course of chemical reactions, which acts to bias the reaction pathway towards products that best relieve the applied mechanical force by directly altering the molecular potential energy surface.⁷⁹ In 2021, Prof. Moore's group demonstrated that external force is an experimental strategy for controlling nonstatistical dynamics and steering reaction trajectories away from constraints imposed by potential energy surfaces.⁸⁰ Their results show that extrinsic force exerted on cyclobutene mechanophores by stretching pendant polymer chains influences product selectivity through force-imparted nonstatistical dynamic effects on the stepwise ring-opening reaction. The high product stereoselectivity is quantified by carbon-13 labeling and is shown to depend on mechanical force, intermediate stability, and reactant stereochemistry. They used computational modeling and simulations to show that, besides altering energy barriers for reaction, the external mechanical force non-statistically activates reactive intramolecular motions, setting up "flyby trajectories" that advance directly to product without isomerization excursions.

6. Theory and modelling for the strength and energy of covalent bonds

6.1. Theoretical framework of covalent bond strength

Eyring *et al.* and Zhurkov initially introduced a phenomenological model that explains how an external force influences the rate of bond dissociation, but is commonly attributed to Bell.^{81–83} Unfortunately, Bell's model operates under the assumption that the potential energy landscape of the reaction remains constant when external force is applied. Consequently, this simplistic, one-dimensional model is only applicable to processes that occur in one dimension—where the force aligns precisely with the reaction coordinate. The tilted potential energy profile model represents an improvement of Bell's model, enabling the structures of reactants and transition states in a reaction to be influenced by external mechanical force. Eyring initially introduced the concept, but it was only when Evans and Ritchie merged this concept with reaction kinetics theory that the description of bond dissociation reactions was fully realized.⁸⁴ In history, experimental investigations into the mechanical stability of covalent bonds have primarily been conducted through ensemble measurements or by inducing long polymer chain fracture in liquids using flow fields.⁸⁵ However, with the advent of atomic force microscopy (AFM) technology, it is now possible to directly measure the real rupture force of single covalent bonds under external loads in micro scale. The force-extension curves obtained during mechanical stretching and relaxation exhibited a wealth

of fingerprint-like features, due to the multiple irreversible steps involved in the rupture process of these single-molecule bridges. For example, a saw-tooth profile is observed when folded and unfolded domains coexist in modular proteins, while a plateau force akin to polymer necking occurs at a single-molecule level during force-coupled ring opening.^{86,87} The rupture forces of covalent bonds are on the order of nanonewtons, and the rupture forces measured for multiple rupture events were also considered in the histogram, which shows the bond rupture probability densities.⁸⁸ Based on DFT calculations, the fracture force for C–C bonds is estimated to be around 3–5 nN.³⁰ However, it should be noted that experimental values tend to slightly underestimate these calculated bond rupture forces.

In general, covalent bond scission between two atoms A and B is modeled within an infinitely long polymer chain in one dimension. The single covalent bond A–B is represented by a suitable analytic potential $V(x)$, that is a Morse potential,⁸⁹ with the minimum of the potential when $x = 0$. The potential $V(x)$ is bonded with the DFT calculations by the physical conditions, $(V_{x \rightarrow \infty}(x) - V(0)) = D$ and $F_{\max}(x) = V'_{\max}$, which show that the analytic potential exhibits the same maximum force and bond dissociation energy as the one from the DFT calculations. So, the Morse potential equation is given by:

$$V = D \left(1 - \exp \left(-\frac{2F_{\max}}{D}x \right)^2 \right) \quad (1)$$

When external mechanical force is applied, the covalent bond is stretched to a distance of x_d given by the condition $F = V'(x_d)$, leading to an effective potential $V_{\text{eff}}(x)$ as depicted in Fig. 6b:

$$V_{\text{eff}}(x) = V(x) - xV'(x_d) \quad (2)$$

The local maximum $V_{\text{eff}}(x_{\text{TS}})$, separating the attractive from the repulsive part of the potential, corresponds to the chemical transition state of a covalent bond rupture event. It is given by:

$$V'(x_{\text{TS}}) = V'(x_d) \quad (3)$$

At a given elongation x_d , the covalent bond scission rate constant $\nu(x_d)$ follows the Arrhenius equation:

$$\nu(x_d) = A(x_d) e^{-E_A(x_d)/kT} \quad (4)$$

For the frequency factor $A(x_d)$, the maximum frequency of an optical phonon in the one-dimensional polymer is chosen, as this corresponds to the motion of A and B in opposite directions and thus to the single covalent bond rupture event:

$$A(x_d) = \frac{1}{2\pi} \sqrt{\frac{2V''(x_d)}{M(A)}} \quad (5)$$

If the activation energy $E_A(x_d)$ is calculated including zero-point correction, it is given that:

$$E_A(x_d) = V_{\text{eff}}(x_{\text{TS}}) - V_{\text{eff}}(x_d) - \frac{1}{2}hA(x_d) \quad (6)$$

The kinetic analysis implies that, unlike, *e.g.*, the energy of a chemical bond, no definitive value exists for its mechanical

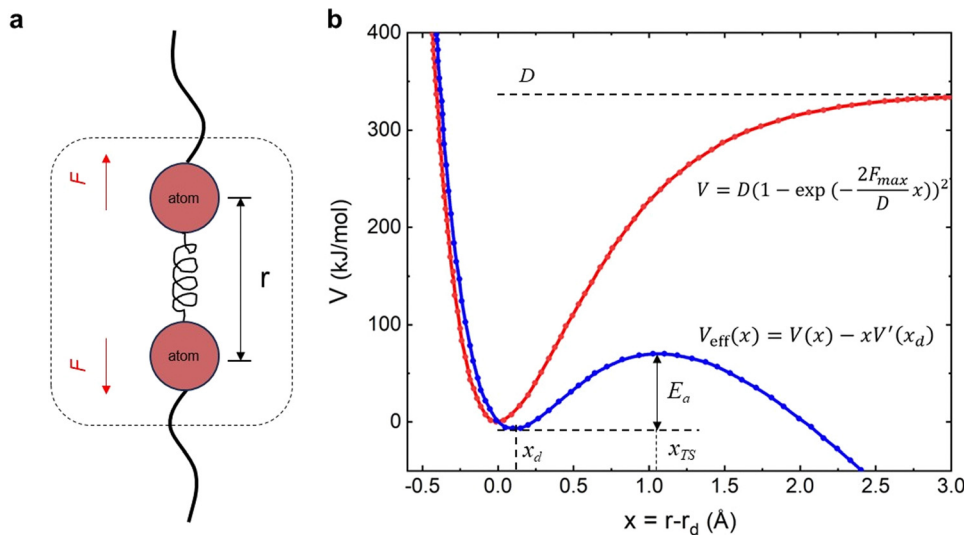


Fig. 6 (a) Schematic illustration for a covalent bond within a polymer chain; (b) undisturbed Morse potential V and effective potential V_{eff} when mechanical force F is applied to the covalent bond.

strength, but that the lifetime of the covalent bond varies as a function of the applied mechanical force.

The central concept of the new framework (explicit external force approach) introduced by Marx and co-workers is the force-transformed potential energy surface (FT-PES),⁹⁰ which given an external constant force, is rigorously defined as

$$V_{\text{EFEI}}(x, F_0) = V_{\text{BO}}(x) - F_0 q(x) \quad (7)$$

where $V_{\text{BO}}(x)$ is the usual Born–Oppenheimer PES as a function of all nuclear cartesian coordinates X , and F_0 is the constant external force associated with some structural parameter q , as it is a generalized coordinate in terms of X . By transforming this formula (7) *via* the Legendre transform, one can show that

$$V_{\text{EFEI}}(F_0) = V_{\text{COGEF}}(q_0) - F_0 q_0 \quad (8)$$

By locating the stationary points of this function, in which the “external force is explicitly included” (EFEI), one can evaluate, without invoking any approximation, properties such as reactant and transition state structures as functions of F_0 .

6.2. Brief introduction of simulation tools

Atomic-scale manipulation with external artificial force has been used to stretch long polymer chains and small molecules in order to study single covalent bond breaks.^{53,91} The mechanical rupture force of the single covalent bond in polymer main chains as a function of bond lifetime can be calculated with an Arrhenius kinetics model based on density functional theory (DFT) calculations and constrained geometries simulate external force (COGEF) theoretical framework. The first computer simulations in this field imposed distance constraint and carried out constraint minimization for different values of this distance showing this way that external force can be simulated by simple geometry constraints—COGEF (constrained geometries simulate external force) that was firstly introduced by

Beyer, which is based on an electronic structure.⁹¹ Briefly, DFT is primarily a theory of the electronic structure of atoms, molecules and solids in their ground states, in which the electronic density distribution $n(r)$ plays the central role.⁹² For a general concept that an external artificial force could be simulated in quantum chemical calculations by geometry constraints and relaxed potential energy surface scans, the abbreviation COGEF for “COnstrained geometries simulate external force” is suggested.

These DFT calculations and COGEF simulations can be performed with the B3LYP/6-31G* level of theory, including one polarization function on each atom, as incorporated in the well-known Gaussian software.^{93,94} The results of the DFT calculations serve as the input for a kinetic model which allows one to calculate the bond rupture rate constant as a function of the applied mechanical force, or the force as a function of the bond lifetime. Moreover, the COGEF method is an operationally simple and highly accessible quantum chemistry technique that enables prediction of mechanochemical reactivity by using another simulation platform named Spartan (Fig. 7a).⁹⁵ In fact, DFT is a semiempirical model for the description of molecular electronic structure. It can't guarantee success in all cases by using DFT to describe chemical bond breaking. Another theoretical approach to simulate the mechanochemical process is external force explicitly included (EFEI),⁹⁶ which enables us to predict structure–reactivity relationships under tension and shows more molecular details of force-to-chemical transduction. It has been demonstrated and confirmed that the EFEI potential is derived from the Legendre transformation of the COGEF potential. In EFEI calculations, in contrast, a constant equal to the external force is added to the nuclear gradient of the appropriate atoms in every step of the geometry optimization (Fig. 7b).⁹⁷ The EFEI method could yield a more exact distortion of the molecular structure, which is in agreement with experiment results.

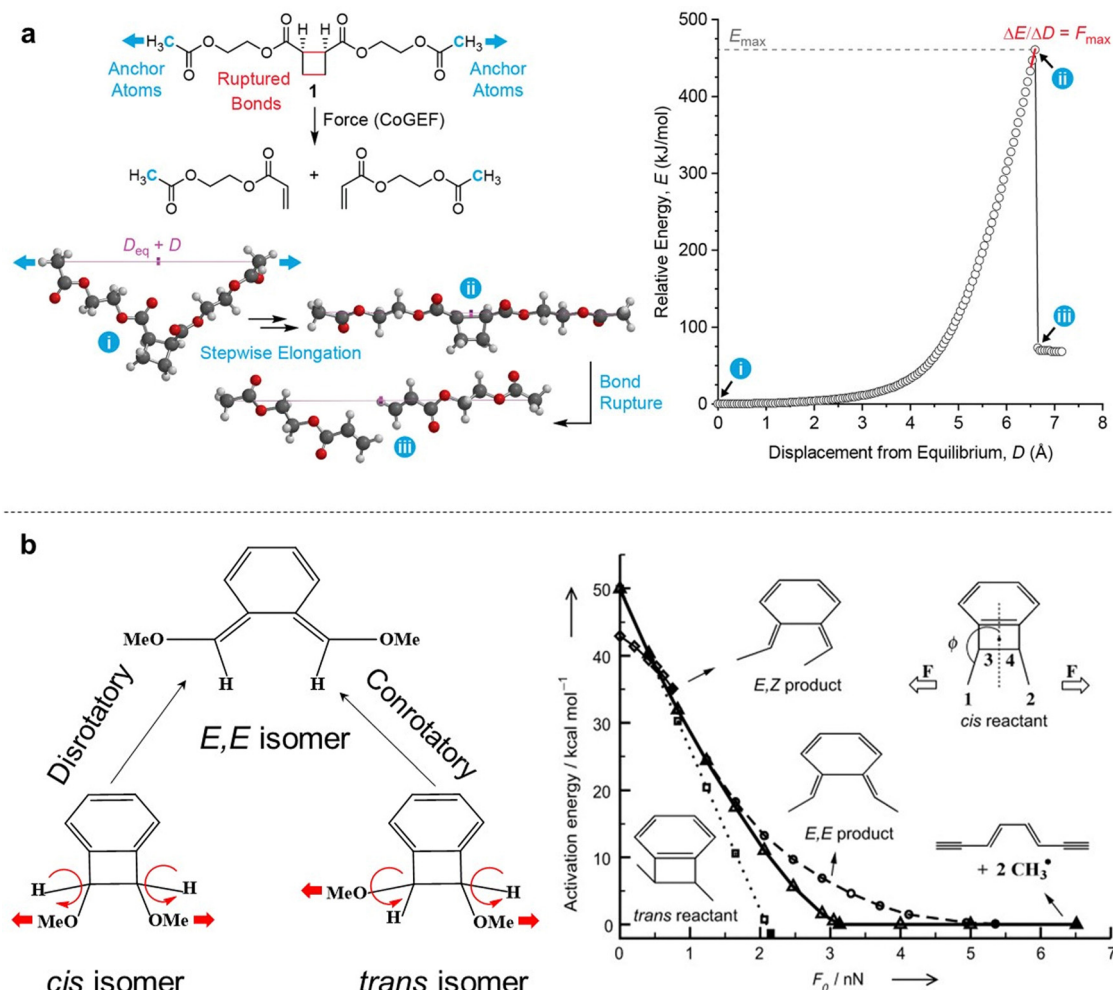


Fig. 7 (a) Illustration of the COGEF method applied to representative cyclobutane mechanophore; Copyright © 2020, American Chemical Society. All rights reserved. (b) Mechanical force induces the opening of strained cyclic mechanophores, force-dependence of the activation energies of the conrotatory (\diamond) and disrotatory (Δ) ring-opening processes of *cis*-1,2-dimethylbenzocyclobutene ("*cis* reactant") as calculated using the EFEI method; Copyright © 2009, Wiley-VCH Verlag GmbH & Co. KGaA, Weinheim. All rights reserved.

7. Summary and outlook

The productive use of destructive mechanical force in polymeric materials has included mechanically induced self-strengthening or self-growing, surface patterning, color/fluorescence change, catalysis and synthesis. Among various stimulation methods, mechanical force acts as a unique vectorial stimulus, which can regulate the mechanoresponse behavior of polymeric materials in terms of both chemical reaction itself and a chemical reaction pathway. These molecular-level chemical reactions ultimately bring about macroscopic changes in the optical, mechanical or surface properties of polymeric materials, thus playing a unique role in damage sensing, stress detection, and materials strengthening. This minireview provides insights into and an understanding of productive mechanochemistry by summarising examples of various productive use of mechanophores, mechanical remodeling of polymeric materials, the development of theoretical concepts, and improved green chemistry metrics compared to those achieved in classical synthetic routes.

We thank our scientific community for their inspiring contributions that have greatly enriched the scientific literature.

Conflicts of interest

The authors declare no competing financial interest.

Acknowledgements

The authors thank Prof. Y. L. Chen, Dr Z. J. Wang, W. Q. Yang and Dr S. Wang for their helpful discussions. Q. F. Mu and J. Hu wrote the manuscript with the help from Prof. Y. L. Chen and Dr S. Wang.

References

- 1 O. Wichterle and D. Lím, *Nature*, 1960, **185**, 117–118.

2 X. Wang, Z. H. Li, S. X. Wang, K. Sano, Z. F. Sun, Z. H. Shao, A. Takeishi, S. Matsubara, D. Okumura, N. Sakai, T. Sasaki, T. Aida and Y. Ishida, *Science*, 2023, **380**, 192–198.

3 M. X. Wang, P. Y. Zhang, M. Shamsi, J. L. Thelen, W. Qian, V. K. Truong, J. Ma, J. Hu and M. D. Dickey, *Nat. Mater.*, 2022, **21**, 359–365.

4 G. J. Lake and A. G. Thomas, *Proc. R. Soc. London, Ser. A*, 1967, **300**, 108–119.

5 L. X. Hou, H. Q. Ju, X. P. Hao, H. K. Zhang, L. Zhang, Z. Y. He, J. J. Wang, Q. Zheng and Z. L. Wu, *Adv. Mater.*, 2023, **35**, 2300244.

6 J. Kim, G. G. Zhang, M. Shi and Z. G. Suo, *Science*, 2021, **374**, 212–216.

7 D. J. Angier and W. F. Watson, *Rubber Chem. Technol.*, 1956, **29**, 1140–1153.

8 K. L. Berkowski, S. L. Potisek, C. R. Hickenboth and J. S. Moore, *Macromolecules*, 2005, **38**, 8975–8978.

9 M. K. Beyer and H. Clausen-Schaumann, *Chem. Rev.*, 2005, **105**, 2921–2948.

10 K. L. Berkowski, S. L. Potisek, C. R. Hickenboth and J. S. Moore, *Macromolecules*, 2005, **38**, 8975–8978.

11 D. Wu, J. M. Lenhardt, A. L. Black, B. B. Akhremitchev and S. L. Craig, *J. Am. Chem. Soc.*, 2010, **132**, 15936–15938.

12 W. M. Huang, X. Wu, X. Gao, Y. F. Yu, H. Lei, Z. S. Zhu, Y. Shi, Y. L. Chen, M. Qin, W. Wang and Y. Cao, *Nat. Chem.*, 2019, **11**, 310–319.

13 H. Staudinger and H. F. Bondy, *Ber. Dtsch. Chem. Ges. B*, 1930, **63**, 734–736.

14 H. Staudinger and W. Hener, *Ber. Dtsch. Chem. Ges. B*, 1934, **67**, 1159–1164.

15 H. Staudinger and E. O. Leupold, *Ber. Dtsch. Chem. Ges. B*, 1930, **63**, 730–733.

16 M. Sakaguchi and J. Sohma, *J. Polym. Sci., Polym. Phys. Ed.*, 1975, **13**, 1233–1245.

17 J. Sohma, *Prog. Polym. Sci.*, 1989, **14**, 451–596.

18 H. Hu, Z. Y. Ma and X. R. Jia, *Mater. Chem. Front.*, 2020, **4**, 3115–3129.

19 M. A. Ghanem, A. Basu, R. Behrou, N. Boechler, A. J. Boydston, S. L. Craig, Y. J. Lin, B. E. Lynde, A. Nelson, H. Shen and D. W. Storti, *Nat. Rev. Mater.*, 2021, **6**, 84–98.

20 B. H. Bowser and S. L. Craig, *Polym. Chem.*, 2018, **9**, 3583–3593.

21 J. Bibas-Ariño and D. Marx, *Chem. Rev.*, 2012, **112**, 5412–5487.

22 M. M. Caruso, D. A. Davis, Q. L. Shen, S. A. Odom, N. R. Sottos, S. R. White and J. S. Moore, *Chem. Rev.*, 2009, **109**, 5755–5798.

23 Y. Yuan and Y. L. Chen, *Chin. J. Polym. Sci.*, 2017, **35**, 1315–1327.

24 Y. C. Simon and S. L. Craig, *Mechanochemistry in materials*, Royal Society of Chemistry, 2017.

25 K. L. Berkowski, S. L. Potisek, C. R. Hickenboth and J. S. Moore, *Macromolecules*, 2005, **38**, 8975–8978.

26 A. L. Black Ramirez, Z. S. Kean, J. A. Orlichi, M. Champhekar, S. M. Elsakr, W. E. Krause and S. L. Craig, *Nat. Chem.*, 2013, **5**, 757–761.

27 J. P. Wang, I. Piskun and S. L. Craig, *ACS Macro Lett.*, 2015, **4**, 834–837.

28 F. Verstraeten, R. Göstl and R. P. Sijbesma, *Chem. Commun.*, 2016, **52**, 8608–8611.

29 T. Matsuda, R. Kawakami, R. Namba, T. Nakajima and J. P. Gong, *Science*, 2019, **363**, 504–508.

30 Z. J. Wang, J. L. Jiang, Q. F. Mu, S. Maeda, T. Nakajima and J. P. Gong, *J. Am. Chem. Soc.*, 2022, **144**, 3154–3161.

31 G. M. Wei, Y. Kudo, T. Matsuda, Z. J. Wang, Q. F. Mu, D. R. King, T. Nakajima and J. P. Gong, *Mater. Horiz.*, 2023, **10**, 4882–4891.

32 K. Seshimo, H. Sakai, T. Watabe, D. Aoki, H. Sugita, K. Mikami, Y. C. Mao, A. Ishigami, S. Nishitsuji, T. Kurose, H. Ito and H. Otsuka, *Angew. Chem., Int. Ed.*, 2021, **60**, 8406–8409.

33 N. Ma, Y. Li, H. P. Xu, Z. Q. Wang and X. Zhang, *J. Am. Chem. Soc.*, 2010, **132**, 442–443.

34 W. Cao, X. L. Zhang, X. M. Miao, Z. M. Yang and H. P. Xu, *Angew. Chem., Int. Ed.*, 2013, **52**, 6233–6237.

35 S. B. Ji, J. H. Xia and H. P. Xu, *ACS Macro Lett.*, 2016, **5**, 78–82.

36 Q. Wu, Y. Yuan, F. Y. Chen, C. X. Sun, H. P. Xu and Y. L. Chen, *ACS Macro Lett.*, 2020, **9**, 1547–1551.

37 X. P. Li, F. Yang, Y. R. Li, C. Liu, P. Zhao, Y. Cao, H. P. Xu and Y. L. Chen, *CCS Chem.*, 2023, **5**, 925–933.

38 Z. Wang, J. Wang, J. Ayarza, T. Steeves, Z. Y. Hu, S. Manna and A. P. Esser-Kahn, *Nat. Mater.*, 2021, **20**, 869–874.

39 Z. Wang, X. J. Zheng, T. Ouchi, T. B. Kouznetsova, H. K. Beech, S. Av-Ron, T. Matsuda, B. H. Bowser, S. Wang, J. A. Johnson, J. A. Kalow, B. D. Olsen, J. P. Gong, M. Rubinstein and S. L. Craig, *Science*, 2021, **374**, 193–196.

40 J. Chung, A. M. Kushner, A. C. Weisman and Z. B. Guan, *Nat. Mater.*, 2014, **13**, 1055–1062.

41 M. Q. Du, H. A. Houck, Q. Yin, Y. W. Xu, Y. Huang, Y. Lan, L. Yang, F. E. Du Prez and G. J. Chang, *Nat. Commun.*, 2022, **13**, 3231.

42 S. Wang, Y. X. Hu, T. B. Kouznetsova, L. Sapir, D. Y. Chen, A. Herzog-Arbeitman, J. A. Johnson, M. Rubinstein and S. L. Craig, *Science*, 2023, **380**, 1248–1252.

43 Q. F. Mu, K. P. Cui, Z. J. Wang, T. Matsuda, W. Cui, H. Kato, S. Namiki, T. Yamazaki, M. Frauenlob, T. Nonoyama, M. Tsuda, S. Tanaka, T. Nakajima and J. P. Gong, *Nat. Commun.*, 2022, **13**, 6213.

44 M. Frauenlob, D. R. King, H. L. Guo, S. Ishihara, M. Tsuda, T. Kurokawa, H. Haga, S. Tanaka and J. P. Gong, *Macromolecules*, 2019, **52**, 6704–6713.

45 M. Frauenlob, H. L. Guo, T. Kurokawa and J. P. Gong, *ACS Macro Lett.*, 2023, **7**, 860–865.

46 Q. F. Mu, Q. S. Zhang, W. Yu, M. L. Su, Z. Y. Cai, K. P. Cui, Y. N. Ye, X. Y. Liu, L. L. Deng, B. J. Chen, N. Yang, L. Chen, L. Tao and Y. Wei, *ACS Appl. Mater. Interfaces*, 2020, **12**, 33152–33162.

47 T. Matsuda, R. Kawakami, T. Nakajima and J. P. Gong, *Macromolecules*, 2020, **53**, 8787–8795.

48 Q. M. Wang, G. R. Gossweiler, S. L. Craig and X. H. Zhao, *Nat. Commun.*, 2014, **5**, 4899.

49 Z. J. Wang, Z. Y. Ma, Y. Wang, Z. J. Xu, Y. Y. Luo, Y. Wei and X. R. Jia, *Adv. Mater.*, 2015, **27**, 6469–6474.

50 Y. H. Mei, W. M. Huang, W. S. Di, X. Zhang, Z. S. Zhu, Y. Y. Zhou, F. W. Hou, W. Wang and Y. Cao, *J. Am. Chem. Soc.*, 2022, **144**, 9949–9958.

51 T. Yamakado and S. Saito, *J. Am. Chem. Soc.*, 2022, **144**, 2804–2815.

52 A. C. Overholts, W. G. Razo and M. J. Robb, *Nat. Chem.*, 2023, **15**, 332–338.

53 D. A. Davis, A. Hamilton, J. L. Yang, L. D. Cremar, D. V. Gough, S. L. Potisek, M. T. Ong, P. V. Braun, T. J. Martínez, S. R. White, J. S. Moore and N. R. Sottos, *Nature*, 2009, **459**, 68–72.

54 C. K. Lee, D. A. Davis, S. R. White, J. S. Moore, N. R. Sottos and P. V. Braun, *J. Am. Chem. Soc.*, 2010, **132**, 16107–16111.

55 G. I. Peterson, M. B. Larsen, M. A. Ganter, D. W. Storti and A. J. Boydston, *ACS Appl. Mater. Interfaces*, 2015, **7**, 577–583.

56 T. S. Wang, N. Zhang, J. W. Dai, Z. L. Li, W. Bai and R. K. Bai, *ACS Appl. Mater. Interfaces*, 2017, **9**, 11874–11881.

57 K. Imato, A. Irie, T. Kosuge, T. Ohishi, M. Nishihara, A. Takahara and H. Otsuda, *Angew. Chem., Int. Ed.*, 2015, **54**, 6168–6172.

58 H. Sakai, T. Sumi, D. Aoki, R. Goseki and H. Otsuka, *ACS Macro Lett.*, 2018, **7**, 1359–1363.

59 Y. L. Chen, A. J. H. Spiering, S. Karthikeyan, G. W. M. Peters, E. W. Meijer and R. P. Sijbesma, *Nat. Chem.*, 2012, **4**, 559–562.

60 W. Yuan, Y. Yuan, F. Yang, M. J. Wu and Y. L. Chen, *Macromolecules*, 2018, **51**, 9019–9025.

61 C. M. Yan, F. Yang, M. J. Wu, Y. Yuan, F. Y. Chen and Y. L. Chen, *Macromolecules*, 2019, **52**, 9376–9382.

62 F. Yang, Y. Yuan, R. P. Sijbesma and Y. L. Chen, *Macromolecules*, 2020, **53**, 905–912.

63 Y. Sagara, M. Karman, E. Verde-Sesto, K. Matsuo, Y. Kim, N. Tamaoki and C. Weder, *J. Am. Chem. Soc.*, 2018, **140**, 1584–1587.

64 R. Kotani, S. Yokoyama, S. P. Nobusue, S. Yamaguchi, A. Osuka, H. Yabu and S. Saito, *Nat. Commun.*, 2022, **13**, 303.

65 R. Göstl and R. P. Sijbesma, *Chem. Sci.*, 2016, **7**, 370–375.

66 Y. Song, K. Lee, W. Hong, S. Cho, H. Yu and C. Chung, *J. Mater. Chem.*, 2012, **22**, 1380–1386.

67 J. P. Wang, T. B. Kouznetsova, R. Boulatov and S. L. Craig, *Nat. Commun.*, 2016, **7**, 13433.

68 X. R. Hu, M. E. McFadden, R. W. Barber and M. J. Robb, *J. Am. Chem. Soc.*, 2018, **140**, 14073–14077.

69 N. Huebsch, C. J. Kearney, X. H. Zhao, J. Kim, C. A. Cezar, Z. G. Suo and D. J. Mooney, *Proc. Natl. Acad. Sci. U. S. A.*, 2014, **111**, 9762–9767.

70 M. B. Larsen and A. J. Boydston, *J. Am. Chem. Soc.*, 2013, **135**, 8189–8192.

71 M. B. Larsen and A. J. Boydston, *J. Am. Chem. Soc.*, 2014, **136**, 1276–1279.

72 C. E. Diesendruck, B. D. Steinberg, N. Sugai, M. N. Silberstein, N. R. Sottos, S. R. White, P. V. Braun and J. S. Moore, *J. Am. Chem. Soc.*, 2012, **134**, 12446–12449.

73 F. Yang, T. Geng, H. Shen, Y. Kou, G. J. Xiao, B. Zou and Y. L. Chen, *Angew. Chem., Int. Ed.*, 2023, e202308662.

74 J. M. J. Paulusse and R. P. Sijbesma, *Angew. Chem., Int. Ed.*, 2004, **43**, 4460–4462.

75 A. Piermattei, S. Karthikeyan and R. P. Sijbesma, *Nat. Chem.*, 2009, **1**, 133–137.

76 P. Michael and W. H. Binder, *Angew. Chem., Int. Ed.*, 2015, **54**, 13918–13922.

77 H. Zhang, F. Gao, X. D. Cao, Y. Q. Li, Y. Z. Xu, W. G. Weng and R. Boulatov, *Angew. Chem., Int. Ed.*, 2016, **55**, 3040–3044.

78 Q. F. Mu, Q. S. Zhang, L. Gao, Z. Y. Chu, Z. Y. Cai, X. Y. Zhang, K. Wang and Y. Wei, *Langmuir*, 2017, **33**, 10291–10301.

79 C. R. Hickenboth, J. S. Moore, S. R. White, N. R. Sottos, J. Baudry and S. R. Wilson, *Nature*, 2007, **446**, 423–427.

80 Y. Liu, S. Holm, J. Meissner, Y. Jia, Q. Wu, T. J. Woods, T. J. Martinez and J. S. Moore, *Science*, 2021, **373**, 208–212.

81 W. Kauzmann and H. Eyring, *J. Am. Chem. Soc.*, 1940, **62**, 3113–3125.

82 S. N. Zhurkov, *Int. J. Fract. Mech.*, 1965, **1**, 311–323.

83 G. I. Bell, *Science*, 1978, **200**, 618–627.

84 E. Evans and K. Ritchie, *Biophys. J.*, 1997, **72**, 1541–1555.

85 A. F. Hron and E. W. Merrill, *Nature*, 2012, **312**, 140–141.

86 H. Clausen-Schaumann, M. Seitz, P. Krautbauer and H. E. Gaub, *Curr. Opin. Chem. Biol.*, 2000, **4**, 524–530.

87 H. Lei, L. Dong, Y. Li, J. S. Zhang, H. Y. Chen, J. H. Wu, Y. Zhang, Q. Y. Fan, B. Xue, M. Qin, B. Chen, Y. Cao and W. Wang, *Nat. Commun.*, 2020, **11**, 4032.

88 M. Granbois, M. Beyer, M. Rief, H. Clausen-Schaumann and H. E. Gaub, *Science*, 1999, **283**, 1727–1730.

89 M. Balsera, S. Stepaniants, S. Izrailev, Y. Oono and K. Schulten, *Biophys. J.*, 1997, **73**, 1281–1287.

90 J. Ribas-Ariño, M. Shiga and D. Marx, *Angew. Chem., Int. Ed.*, 2009, **48**, 4190–4193.

91 M. K. Beyer, *J. Chem. Phys.*, 2000, **112**, 7307–7312.

92 D. S. Sholl, *Density functional theory: a practical introduction*, John Wiley & Sons, Inc., 2009.

93 J. L. Jiang, K. Kubota, M. Jin, Z. J. Wang, T. Nakajima, H. Ito, J. P. Gong and S. Maeda, *ChemRxiv*, 2022, preprint, DOI: [10.26434/chemrxiv-2022-fr091](https://doi.org/10.26434/chemrxiv-2022-fr091).

94 M. J. Kryger, A. M. Munaretto and J. S. Moore, *J. Am. Chem. Soc.*, 2011, **133**, 18992–18998.

95 I. M. Klein, C. C. Husic, D. P. Kovács, N. J. Choquette and M. J. Robb, *J. Am. Chem. Soc.*, 2020, **142**, 16364–16381.

96 P. Dopieralski, J. Ribas-Ariño and D. Marx, *Angew. Chem., Int. Ed.*, 2011, **50**, 7105–7108.

97 Y. Y. Sun, I. Kevlishvili, T. B. Kouznetsova, Z. P. Burke, S. L. Craig, H. J. Kulik and J. S. Moore, *ChemRxiv*, 2023, preprint, DOI: [10.26434/chemrxiv-2023-rzwhn](https://doi.org/10.26434/chemrxiv-2023-rzwhn).